Multi-trait Polygenic Probability Risk Score Enhances Glaucoma Prediction Across Ancestries

Xiaoyi Raymond Gao[1,2]

[1]Department of Ophthalmology and Visual Sciences, The Ohio State University, Columbus, OH 43210, USA

[2]Department of Biomedical Informatics, The Ohio State University, Columbus, OH 43210, USA

[*]Correspondence should be addressed to:
Xiaoyi Raymond Gao, PhD
Associate Professor
Department of Ophthalmology and Visual Sciences
Department of Biomedical Informatics
The Ohio State University
Columbus, OH 43212
USA
Phone: (614) 293-5287
Fax: (614) 293-5602
Email: raymond.gao@osumc.edu

Abstract:

Primary open-angle glaucoma (POAG) remains the leading cause of irreversible blindness worldwide, with early detection crucial for preventing vision loss. However, current risk assessment methods have limited predictive power. Here, we present a multi-trait polygenic probability risk score (PPRS) approach that integrates multiple glaucoma-related traits and leverages functional genomic annotations to enhance POAG prediction across diverse ancestries. We constructed PRSs for POAG, intraocular pressure (IOP), vertical cup-to-disc ratio (VCDR), and retinal nerve fiber layer (RNFL) thickness using extensive genomic coverage (>7 million variants) and 96 functional annotations through the SBayesRC method. Validation in the UK Biobank (n=324,713, European ancestry) and Mexican American Glaucoma Genetic Study (MAGGS, n=4,549, Latino ancestry) demonstrated significant improvements in predictive accuracy over conventional approaches. Our multi-trait PPRS achieved area under the curve (AUC) values of 0.814 in Europeans and 0.801 in Latinos, compared to AUC ≤0.79 for single-trait models. We identified ancestry-specific differences in genetic contributions, with IOP demonstrating the strongest association in Europeans (OR=1.63, $P = 5.37 \times 10^{-89}$), while VCDR was predominant in Latinos (OR=1.64, $P = 2.04 \times 10^{-11}$). The model achieved remarkable risk stratification, with the highest PPRS decile showing 80.2-fold and 51.1-fold increased POAG risk in Europeans and Latinos, respectively, compared to the lowest decile. Importantly, the top PPRS quintile captured 65.9% and 62.2% of POAG cases in Europeans and Latinos, substantially improving upon previous approaches. Our findings demonstrate that integrating multiple disease-relevant traits and functional annotations significantly enhances polygenic prediction of POAG across diverse populations, with significant implications for targeted screening, early intervention, and reduction of disease burden.

Keywords:

glaucoma, polygenic risk score, genetic prediction, multi-ancestry, precision medicine

Introduction

Glaucoma is the leading cause of irreversible blindness[1, 2], affecting about 80 million individuals worldwide[3, 4], with primary open-angle glaucoma (POAG) constituting approximately 90% of glaucoma cases in North America[4, 5]. Despite available treatments to slow disease progression, the irreversible nature of glaucoma-induced vision loss underscores the critical importance of early detection and intervention. While traditional risk assessment relies primarily on clinical measurements and family history, recent advances in genomics offer promising opportunities for enhanced risk stratification.

Polygenic risk scores (PRSs) have emerged as powerful tools for quantifying genetic predisposition to complex diseases[6-8]. However, their application to POAG has faced three key limitations. First, previous studies utilizing single-trait PRSs have achieved limited stratification ability, with about 50% of cases being identified in the top PRS quintile in a recent report[9]. Second, existing approaches have failed to capture the inherent complexity of POAG's pathophysiology, which involves multiple quantitative endophenotypes[1, 10], including intraocular pressure (IOP), vertical cup-to-disc ratio (VCDR), and retinal nerve fiber layer (RNFL) thickness. Though the multi-trait analysis of genome-wide association studies (MTAG) approach can analyze multi-traits jointly, previous studies indicated MTAG-derived PRS did not provide the optimal prediction accuracy for POAG[11]. For POAG PRS prediction per se, these endophenotypes may be best modeled separately in PRS prediction. Third, most POAG PRS prediction studies have employed limited genomic coverage (< 1M markers) and have lacked integration of functional annotations, potentially missing important biological signals. These limitations underscore the necessity for more advanced models that can capture the multifaceted genetic underpinnings of POAG.

Here, we present a multi-trait polygenic probability risk score (PPRS) approach, integrating PRSs derived from different modalities, including imaging-derived phenotypes, that addresses these limitations through three key innovations: 1) integrating multiple disease-relevant quantitative traits into PRS model-

74 ing; 2) incorporating extensive genomic coverage (over seven million variants) and 96 functional annota-
75 tions; 3) validating across diverse ancestral populations. We hypothesized that this comprehensive ap-
76 proach would significantly improve POAG risk prediction across diverse populations compared to exist-
77 ing methods. To test this hypothesis, we evaluated our model in two independent cohorts: the UK Bi-
78 obank (UKB) for European ancestry individuals and the Mexican American Glaucoma Genetic Study
79 (MAGGS) for Latino participants.
80
81 **Methods**
82 *Study Design and Populations*
83 We conducted a two-stage study: first, deriving genome-wide association study (GWAS) summary statis-
84 tics from previously published data and our own GWAS analyses (details provided below); second, vali-
85 dating PRSs in a subset of the UKB cohort (n = 324,713, POAG cases: 2,168) and the MAGGS cohort (n
86 = 4,549, POAG cases: 275), both independent of the GWAS discovery samples. UKB and MAGGS re-
87 ceived approval from respective institutional review boards[12-14]. All participants provided written in-
88 formed consent. The study adhered to the tenets of the Declaration of Helsinki. We obtained fully de-
89 identified data to ensure participant confidentiality.
90
91 *UKB dataset*
92 The UKB is an ongoing, large-scale prospective cohort study with over 500,000 adult participants aged
93 40 to 69 at enrollment (2006–2010), registered with the National Health Service in the United Kingdom[12,
94 13]. The study collected medical information, lifestyle data, and DNA samples, including ophthalmologic
95 data for a subset of approximately 118,000 participants. Our access and use of the UKB data were ap-
96 proved under application #23424. Our analysis focused on participants of European ancestry. Genotyping
97 was performed using the UK BiLEVE Axiom Array or the UKB Axiom Array, with imputation based on
98 reference panels from the 1000 Genomes Project (1KGP), UK10K, and the Haplotype Reference Consor-
99 tium (HRC)[15]. Variants with an imputation INFO score less than 0.3 and minor allele frequency less than

100 0.01 were excluded, resulting in approximately 10.3 million variants for downstream analysis. For indi-
101 viduals with IOP measurements and RNFL data, we conducted IOP analyses[16] and a GWAS of RNFL to
102 derive summary statistics. For those without ophthalmic exams (n = 324,713, unrelated, independent of
103 the IOP and RNFL GWAS samples)[17], we utilized their data for PRS construction and association testing
104 with POAG. POAG (H40.1) cases were identified using the International Classification of Diseases Tenth
105 Revision (ICD-10) codes. Controls were identified as those who did not have glaucoma.
106
107 *MAGGS dataset*
108 MAGGS samples were sourced from the Los Angeles Latino Eye Study (LALES)[18], a population-based
109 epidemiologic study examining visual impairment and ocular diseases in 6,357 Latino individuals aged
110 40 or older in Los Angeles County, California. The presence of POAG was determined by agreement
111 among three glaucoma specialists using clinical data, including the presence of open angles, characteristic
112 visual field abnormalities, and optic disc damage in at least one eye. MAGGS and LALES genotyped
113 4,996 Latino individuals using either the Illumina OmniExpress BeadChip or the Illumina Hispanic/SOL
114 BeadChip[14, 19]. Imputation was performed using 1KGP reference panel, excluding variants with a Mach[20]
115 Rsq less than 0.3 and minor allele frequency less than 0.01, resulting in approximately 9.9 million im-
116 puted variants. Our analysis included 4,549 participants (4,108 unrelated and 441 related individuals)
117 from this dataset.
118
119 *GWAS summary statistics*
120 We used previously published GWAS summary statistics for POAG, IOP, and vertical cup-to-disc ratio
121 (VCDR), as well as our own GWAS results for RNFL. The details are as follows:
122 1) POAG: We used GWAS results from Gharahkhani et al. (2021), which performed a multi-eth-
123 nic meta-analysis using the International Glaucoma Genetics Consortium (IGGC) and UKB datasets,
124 comprising 383,500 individuals of European, Asian, and African descent[21]. For building PRSs for UKB

125 participants, we used results from IGGC only, excluding UKB individuals, resulting in a cross-ancestry
126 meta-analysis with 192,702 individuals suitable for UKB PRS construction.
127 2) IOP: We used GWAS results from Gao et al. (2018), including 115,486 UKB participants of
128 European ancestry[16].
129 3) VCDR: We used GWAS summary statistics from Han et al. (2021), involving 111,724 individ-
130 uals of European and Asian descent from UKB, the Canadian Longitudinal Study on Aging (CLSA), and
131 IGGC[22]. VCDR measurements were obtained from human graders and deep learning models applied to
132 retinal fundus images.
133 4) RNFL: We conducted a GWAS with 52,902 European ancestry UKB participants using the
134 REGENIE[23] software and RNFL thickness values derived from optical coherence tomography images[24].
135 We excluded outliers and low-quality images (image quality score less than 45). We averaged RNFL val-
136 ues between the left and right eyes and applied rank-based inverse normalization. We adjusted for age,
137 sex, diabetes, spherical equivalent, and the first 10 principal components of genetic ancestry. Supplemen-
138 tary Figure 1 presents a Manhattan plot of the genome-wide -log10(*P* values) for our RNFL GWAS anal-
139 ysis.
140 These summary statistics provided the foundation for constructing PRSs in our analysis, tailored to differ-
141 ent phenotypes relevant to POAG risk.
142
143 *PRS construction*
144 We employed three different approaches to construct PRSs:
145 First, we implemented a traditional clumping and thresholding (C+T) based PRS[25] using
146 PLINK[26, 27] to construct the POAG PRS, denoted as PRS-POAG-C+T. Independent single nucleotide pol-
147 ymorphisms (SNPs) were identified using linkage disequilibrium (LD)-based clumping ($r^2 < 0.3$) and se-
148 lected based on a p-value threshold of $P < 5 \times 10^{-5}$.
149 Second, we constructed enhanced PRSs using the SBayesRC[28] method, which leverages func-
150 tional genomic annotations and extensive SNP coverage to improve polygenic risk prediction for complex

151 traits or diseases. By integrating 96 functional annotations, including regulatory elements, chromatin
152 states, and transcription factor binding sites, and analyzing over seven million SNPs, we sought to sub-
153 stantially improve PRS accuracy. Using SBayesRC, we constructed PRSs for POAG (PRS-POAG), IOP
154 (PRS-IOP), VCDR (PRS-VCDR), and RNFL thickness (PRS-RNFL).

155 Third, we constructed a MTAG-derived PRS for POAG to enable direct comparison. We utilized
156 summary statistics for 2,763 uncorrelated SNPs (identified through LD clumping at $r^2 = 0.1$ and a signifi-
157 cance threshold of $P < 0.001$) from Craig et al.'s (2020) MTAG analysis[29]. The MTAG-derived PRS was
158 calculated using the formula: PRS-POAG-MTAG(i) = $\sum \beta_j G_{ij}$, where β_j represents the regression coeffi-
159 cient for SNP_j, and G_{ij} indicates the risk allele dosage for SNP_j in individual i. Given that Craig et al. used
160 UKB participants in their MTAG analysis, we avoided applying the MTAG-derived PRS to UKB partici-
161 pants to prevent potential data leakage. Consequently, this PRS was exclusively applied to MAGGS study
162 participants.

163 All constructed PRSs were standardized to have a mean of zero and a variance of one.

164

165 *Statistical analysis*

166 To evaluate the association between PRSs and POAG, we performed logistic regression analyses adjusted
167 for age and sex. We assessed the predictive ability of the PRSs for POAG using AUC. For unrelated sam-
168 ples, we employed leaving-one-out cross-validation to obtain predicted probabilities of POAG for each
169 individual. For MAGGS related samples, predictive models were developed using MAGGS unrelated
170 samples and subsequently applied to the related individuals to derive predicted probabilities. We termed
171 this derived probability measure as polygenic probability risk score (PPRS), integrating multiple PRSs
172 through statical modeling, to differentiate it from traditional single-trait PRSs and the MTAG-derived
173 PRS. To check potential multicollinearity among PRSs, we used two complementary approaches. First,
174 we computed the variance inflation factor (VIF) for each predictor, noting that VIF values less than 5 typ-
175 ically indicate low correlation[30]. Second, we employed XGBoost[31], a tree-based method known to be less
176 sensitive to collinearity, and examined feature importances via SHapley Additive exPlanations (SHAP)

177 values[32], following our previous methodology[33]. For risk stratification, we divided the PPRS into deciles
178 and compared the odds of POAG among study participants in higher PPRS deciles versus those in the
179 lowest PPRS decile in both the UKB and MAGGS datasets. A statistical significance threshold of $P <$
180 0.05 was used for all analyses. All analyses and plots were performed using R version 4.4, SAS version
181 9.4, and Python version 3.12.
182
183 **Results**
184 Table 1 summarizes the characteristics of the study samples from the UK Biobank (UKB) and the Mexi-
185 can American Glaucoma Genetic Study (MAGGS). The UKB cohort comprised 324,713 individuals with
186 2,168 glaucoma cases and 322,545 controls. The mean (standard deviation [SD]) age of glaucoma and
187 non-glaucoma were 63.0 (5.7) and 57.1 (8.0) years, respectively. Females consisted of 48.4% and 54.3%
188 in glaucoma and non-glaucoma participants, respectively. The MAGGS dataset included 4,549 partici-
189 pants with 275 glaucoma cases and 4,274 controls. The mean (SD) age of glaucoma and non-glaucoma
190 were 66.4 (11.1) and 56.1 (10.2), respectively. Females constituted 52.4% and 59.2% of glaucoma and
191 non-glaucoma participants, respectively.
192
193 Table 2 presents the results of the single PRS logistic regression analyses, adjusted for age and sex,
194 among UKB and MAGGS participants. In the UKB cohort (Table 2a), the traditional clumping and
195 thresholding (C+T) method PRS for POAG (PRS-POAG-C+T) yielded an odds ratio (OR) of 1.71 (95%
196 confidence interval [CI]: 1.64–1.79; $P = 8.71 \times 10^{-141}$). The SBayesRC-derived PRS for POAG (PRS-
197 POAG) showed a stronger association with an OR of 2.14 (95% CI: 2.05–2.24; $P = 8.54 \times 10^{-269}$). The
198 SBayesRC-derived PRSs for IOP (PRS-IOP), VCDR (PRS-VCDR), and RNFL thickness (PRS-RNFL)
199 also demonstrated significant associations with POAG. Both PRS-POAG and PRS-IOP gave similar AUC
200 (0.79) for predicting glaucoma. Similarly, in the MAGGS cohort (Table 2b), the PRS-POAG-MTAG had
201 a lower OR of 1.44 (95% CI: 1.24–1.60; $P = 1.17 \times 10^{-7}$) and a lower AUC of 0.75 (95% CI: 0.72–0.78).
202 PRS-VCDR showed the highest OR of 1.90 (95% CI: 1.66-2.17; $P = 1.39 \times 10^{-20}$) and the highest AUC

203 of 0.78 (95% CI: 0.75-0.81). The PRS-POAG-C+T, PRS-IOP, PRS-POAG, and PRS-RNFL in MAGGS
204 participants also exhibited significant associations with POAG.
205
206 Table 3 displays the results of the multiple PRS logistic regression analyses, assessing the combined
207 association of PRSs with POAG and their relative importance in each cohort. In the UKB participants,
208 PRS-POAG had an OR of 1.59 ($P = 1.23 \times 10^{-74}$), PRS-IOP showed the strongest association with an OR
209 of 1.63 ($P = 5.37 \times 10^{-89}$), PRS-VCDR had an OR of 1.28 ($P = 1.99 \times 10^{-27}$), and PRS-RNFL exhibited
210 an OR of 0.94 ($P = 0.002$), indicating a slight inverse association (larger PRS-RNFL indicated thicker
211 RNFL and hence is protective). The OR for a simultaneous one-SD-unit-increase in all four standardized
212 PRS variables was 3.11 (95% CI: 2.89-3.34). In the MAGGS cohort, PRS-POAG had an OR of 1.40 ($P =$
213 7.63×10^{-5}), PRS-IOP an OR of 1.15 ($P = 0.07$), PRS-VCDR showed the strongest association with an
214 OR of 1.64 ($P = 2.04 \times 10^{-11}$), and PRS-RNFL had an OR of 0.85 ($P = 0.016$), also suggesting an inverse
215 relationship. The OR for a simultaneous one-SD-unit-increase in all four standardized PRS variables was
216 2.25 (95% CI: 1.79-2.82). These results highlight the significant contributions of the different PRSs in
217 predicting POAG risk in both cohorts. Notably, PRS-IOP contributed most significantly to POAG risk
218 prediction in the UKB dataset, whereas PRS-VCDR had the strongest contribution in the MAGGS da-
219 taset.
220
221 To evaluate potential collinearity among these PRSs (PRS-POAG, PRS-IOP, PRS-VCDR, and PRS-
222 RNFL), we applied two complementary approaches: (1) VIF analysis and (2) XGBoost with SHAP-based
223 feature importance. Supplementary Table 1 presents the VIF values for each predictor in the logistic re-
224 gression models. These values are only slightly above 1, indicating minimal collinearity, and all remain
225 well below the typical cutoff of 5. Supplementary Figure 2 displays the SHAP feature importance rank-
226 ings from our XGBoost models. In UKB participants, PRS-IOP and PRS-POAG both rank highly among

227 the PRSs. In MAGGS, PRS-VCDR shows the highest importance among the PRSs, aligning with the lo-
228 gistic regression findings. Collectively, these results underscore the validity and robustness of our logistic
229 regression analyses.
230
231 We examined the discriminatory ability of the PRSs (PRS-POAG, PRS-IOP, PRS-VCDR, and PRS-
232 RNFL) for predicting POAG using leave-one-out cross-validation logistic regression models and calcu-
233 lated AUC. Figure 1 illustrates these results. In UKB participants (Figure 1A), the baseline model includ-
234 ing only age and sex had an AUC of 0.711. Adding PRS-POAG-C+T increased the AUC to 0.761, while
235 incorporating the SBayesRC-derived PRS-POAG improved it to 0.790, a 3% increase over the C+T ap-
236 proach ($P = 2.31 \times 10^{-29}$). Incorporating all four PRSs (PRS-POAG, PRS-IOP, PRS-VCDR, and PRS-
237 RNFL) with adjustment for age and sex resulted in an AUC of 0.814 (95% CI: 0.805–0.822), representing
238 a 10.3% improvement over the baseline model ($P = 4.37 \times 10^{-135}$). In MAGGS participants (Figure 1B),
239 the baseline AUC was 0.746, which increased to 0.760 with PRS-POAG-MTAG, to 0.773 with PRS-
240 POAG-C+T and to 0.782 with PRS-POAG. The full model with all four PRSs (PRS-POAG, PRS-IOP,
241 PRS-VCDR, and PRS-RNFL) achieved an AUC of 0.801 (95% CI: 0.775–0.828), providing a 5.5% en-
242 hancement over the baseline model ($P = 3.05 \times 10^{-7}$). These findings indicate that incorporating multiple
243 glaucoma-related PRSs significantly improves the prediction of POAG in both cohorts.
244
245 We further evaluated POAG risk stratification using PPRS from our leave-one-out logistic regression
246 models, which aggregate the effects of age, sex, the PRSs of POAG, IOP, VCDR, and RNFL and predict
247 on the leave-one-out sample. Analysis of PPRS revealed strong risk stratification capabilities (Figure 2).
248 In the UKB cohort (Figure 2A), clear trend emerged with increasing ORs across higher PPRS deciles. In-
249 dividuals in the highest decile had 80.24-fold increased odds of POAG (95% CI: 46.42–138.69; $P = 1.53$
250 $\times 10^{-55}$) compared to those in the lowest decile. Similarly, in the MAGGS cohort (Figure 2B), participants
251 in the highest decile demonstrated 51.11-fold increased odds of POAG (95% CI: 16.11–162.11; $P = 2.43$
252 $\times 10^{-11}$) compared to the lowest decile. Most POAG cases (46.63% in UKB and 41.82% in MAGGS) are

253 in the highest decile category of PPRS (supplementary Table 2). Notably, when examining the top quin-
254 tile of PPRS, we identified 65.95% and 62.2% of POAG cases for Europeans and Latinos, respectively,
255 representing a substantial improvement over previous approaches. Take together, these findings under-
256 score the strong relationship between PPRS deciles and POAG risk across UKB and MAGGS, highlight-
257 ing the potential utility of the PPRS for risk stratification in clinical settings.
258
259 **Discussion**
260 Our study demonstrates that integrating multiple glaucoma-related traits with functional annotations sub-
261 stantially improves the polygenic prediction for POAG across diverse ancestries. Three key findings
262 emerge from our analysis: First, our multi-modal PPRS approach achieved higher predictive accuracy,
263 with AUC values of 0.814 in Europeans and 0.801 in Latinos, compared to our single-trait models (AUC
264 $\leq$ 0.79). This improvement likely reflects the complex genetic architecture of POAG, where multiple bio-
265 logical pathways contribute to disease development. Second, we identified ancestry-specific differences
266 in the relative contributions of component PRSs. In Europeans, IOP showed the strongest association,
267 whereas VCDR was most strongly associated in Latinos. This finding underscores the importance of pop-
268 ulation-specific risk assessment and suggests distinct genetic mechanisms underlying POAG across an-
269 cestral groups. Third, the strong risk stratification achieved by our PPRS, demonstrating over 80-fold and
270 51-fold risk differences between extreme deciles in Europeans and Latinos, respectively, suggests signifi-
271 cant clinical utility. This high level of stratification can effectively identify individuals at greatest risk
272 who might benefit from enhanced screening and early intervention.
273
274 Direct comparison with previous glaucoma PRS studies is challenging due to differences in target
275 datasets. However, several observations can be highlighted. First, the correlation between phenotypes is
276 not equivalent to correlations among PRSs. Despite high phenotypic correlations among POAG, IOP, and
277 VCDR[34], correlations among the corresponding PRSs are notably lower based on our VIF analysis. By
278 incorporating quantitative traits like IOP, VCDR, and RNFL thickness into a unified PPRS framework,

279 we effectively address the heterogeneous nature of POAG. Each of these traits reflects distinct biological
280 mechanisms and provides unique predictive information, enhancing the model's capability to capture
281 overall glaucoma risk. Second, MTAG-derived PRS has not yielded optimal prediction accuracy for
282 POAG, as demonstrated in recent studies[11]. Although several recent reports employed lassosum for PRS
283 construction [9, 35-38], previous methodological evaluations indicate that lassosum does not achieve optimal
284 predictive performance[11, 39]. We employed the SBayesRC approach, which integrates functional genomic
285 annotations to prioritize biologically relevant variants, leveraging millions of SNPs. This method offers
286 marked advantages over conventional PRS methodologies[28]. These improvements in polygenic risk esti-
287 mation have substantial implications for effective sample stratification.
288
289 One of the most direct clinical applications of PRS is identifying high-risk individuals. MacGregor et
290 al. (2018), using an IOP PRS, reported an increased glaucoma risk (OR = 5.6, 95% CI: 4.1–7.6) compar-
291 ing the top and bottom deciles[40]. Craig et al. (2020), employing an MTAG approach for their POAG PRS,
292 observed a higher OR of 14.9 (95% CI: 10.7–20.9) for comparing the top and bottom deciles[29]. Gao et al.
293 (2019) found an OR of 6.3 for their top IOP PRS quintile versus the bottom quintile comparison and ap-
294 proximately 40.6% of POAG cases were found in the top quintile[17], while de Vries et al. (2025) identified
295 about 50% in their top glaucoma PRS quintile[9]. Our study substantially improves upon these results,
296 demonstrating ORs of 80.2 (95% CI: 46.4–138.7) in Europeans and 51.1 (95% CI: 16.1–162.1) in Latinos
297 when comparing extreme deciles of our PPRS. Additionally, we identified 65.9% and 62.2% of glaucoma
298 cases within the top quintile of our PPRS scores for Europeans and Latinos (supplementary Table 2), re-
299 spectively, underscoring significant advancement in polygenic prediction performance relative to previ-
300 ous studies.
301
302 Our study has several strengths, notably the use of a comprehensive multi-trait PPRS approach that
303 integrates multiple glaucoma-related traits, including imaging-derived ones, and leverages functional an-
304 notations (through SBayesRC) to improve prediction accuracy. By evaluating PRS performance in both

305 European and Latino populations, we address the crucial need for inclusive and representative genetic re-
306 search, especially among traditionally understudied groups[41]. However, our study also has limitations.
307 Due to resource constraints, we included only European and Latino populations in this study. Expanding
308 future research to additional populations would enhance generalizability and ensure broader applicability
309 of our findings. Furthermore, our PRS construction was limited to common variants. Incorporating rare
310 variants, similar to previous reports on rare variants associated with IOP[42], warrants further investigation.
311
312 We utilized logistic regression for our statistical modeling, providing interpretable outcomes suitable
313 for analyzing associations between PRSs and glaucoma. Nonetheless, prediction accuracy might be fur-
314 ther improved through advanced machine learning techniques. For example, gradient boosting methods
315 like XGBoost, which we have successfully applied in related studies[33], could potentially capture more
316 complex non-linear interactions. However, the implementation of these machine learning techniques typi-
317 cally requires more complex hyperparameter tuning and computational resources. Future research could
318 explore the potential of these advanced modeling techniques while balancing their complexity with inter-
319 pretability and practical application.
320
321 In conclusion, our multi-trait PPRS approach, combining multiple glaucoma-related traits and incor-
322 porating functional annotations, represents a significant advancement in polygenic risk prediction for
323 POAG. The robust performance across different ancestral groups and substantial risk stratification capa-
324 bilities suggest considerable potential for enhancing early detection and preventative strategies. By facili-
325 tating the identification of individuals at high genetic risk, our approach has significant implications for
326 timely clinical intervention and could ultimately reduce the public health burden of POAG.
327

Acknowledgements

We would like to thank the study participants from the UK Biobank, the Los Angeles Latino Eye Study, the Mexican American Glaucoma Genetic Study, and the staff who aided in data collection and processing. This work was supported in part by National Institutes of Health (NIH; Bethesda, MD, USA) grants P30EY032857 and R01EY022651. The content is solely the responsibility of the authors and does not necessarily represent the official views of the NIH.

References

1. Fan BJ, Wiggs JL. Glaucoma: genes, phenotypes, and new directions for therapy. J Clin Invest 2010;120(9):3064-72.
2. Blindness GBD, Vision Impairment C, Vision Loss Expert Group of the Global Burden of Disease S. Causes of blindness and vision impairment in 2020 and trends over 30 years, and prevalence of avoidable blindness in relation to VISION 2020: the Right to Sight: an analysis for the Global Burden of Disease Study. Lancet Glob Health 2021;9(2):e144-e60.
3. Weinreb RN, Leung CK, Crowston JG, et al. Primary open-angle glaucoma. Nat Rev Dis Primers 2016;2:16067.
4. Tham YC, Li X, Wong TY, et al. Global prevalence of glaucoma and projections of glaucoma burden through 2040: a systematic review and meta-analysis. Ophthalmology 2014;121(11):2081-90.
5. Lang GK. Ophthalmology: A Pocket Textbook Atlas, 2nd ed. Stuttgart, New Yok: Thieme 2007.
6. Purcell SM, Wray NR, Stone JL, et al. Common polygenic variation contributes to risk of schizophrenia and bipolar disorder. Nature 2009;460(7256):748-52.
7. Kachuri L, Chatterjee N, Hirbo J, et al. Principles and methods for transferring polygenic risk scores across global populations. Nat Rev Genet 2024;25(1):8-25.
8. Torkamani A, Wineinger NE, Topol EJ. The personal and clinical utility of polygenic risk scores. Nat Rev Genet 2018;19(9):581-90.
9. de Vries VA, Hanyuda A, Vergroesen JE, et al. The Clinical Usefulness of a Glaucoma Polygenic Risk Score in 4 Population-Based European Ancestry Cohorts. Ophthalmology 2025;132(2):228-37.
10. Ramdas WD, Amin N, van Koolwijk LM, et al. Genetic architecture of open angle glaucoma and related determinants. J Med Genet 2011;48(3):190-6.
11. Biradar M, Luben R, Stuart K, et al. Comparison of multiple polygenic risk score derivation approaches for population-level prediction of primary open-angle glaucoma. Investigative Ophthalmology & Visual Science 2023;64(8):492-.
12. Sudlow C, Gallacher J, Allen N, et al. UK biobank: an open access resource for identifying the causes of a wide range of complex diseases of middle and old age. PLoS Med 2015;12(3):e1001779.
13. Allen NE, Sudlow C, Peakman T, et al. UK biobank data: come and get it. Sci Transl Med 2014;6(224):224ed4.
14. Nannini DR, Torres M, Chen YI, et al. A Genome-Wide Association Study of Vertical Cup-Disc Ratio in a Latino Population. Invest Ophthalmol Vis Sci 2017;58(1):87-95.
15. Bycroft C, Freeman C, Petkova D, et al. The UK Biobank resource with deep phenotyping and genomic data. Nature 2018;562(7726):203-9.
16. Gao XR, Huang H, Nannini DR, et al. Genome-wide association analyses identify new loci influencing intraocular pressure. Hum Mol Genet 2018;27(12):2205-13.
17. Gao XR, Huang H, Kim H. Polygenic Risk Score Is Associated With Intraocular Pressure and Improves Glaucoma Prediction in the UK Biobank Cohort. Transl Vis Sci Technol 2019;8(2):10.
18. Varma R, Paz SH, Azen SP, et al. The Los Angeles Latino Eye Study: design, methods, and baseline data. Ophthalmology 2004;111(6):1121-31.
19. Nannini D, Torres M, Chen YD, et al. African Ancestry Is Associated with Higher Intraocular Pressure in Latinos. Ophthalmology 2016;123(1):102-8.
20. Li Y, Abecasis GR. Mach 1.0: Rapid haplotype reconstruction and missing genotype inference. Am J Hum Genet 2006;S79.
21. Gharahkhani P, Jorgenson E, Hysi P, et al. Genome-wide meta-analysis identifies 127 open-angle glaucoma loci with consistent effect across ancestries. Nat Commun 2021;12(1):1258.
22. Han X, Steven K, Qassim A, et al. Automated AI labeling of optic nerve head enables insights into cross-ancestry glaucoma risk and genetic discovery in >280,000 images from UKB and CLSA. Am J Hum Genet 2021.
23. Mbatchou J, Barnard L, Backman J, et al. Computationally efficient whole-genome regression for quantitative and binary traits. Nat Genet 2021;53(7):1097-103.

24. Ko F, Foster PJ, Strouthidis NG, et al. Associations with Retinal Pigment Epithelium Thickness Measures in a Large Cohort: Results from the UK Biobank. Ophthalmology 2017;124(1):105-17.
25. Prive F, Vilhjalmsson BJ, Aschard H, Blum MGB. Making the Most of Clumping and Thresholding for Polygenic Scores. Am J Hum Genet 2019;105(6):1213-21.
26. Purcell S, Neale B, Todd-Brown K, et al. PLINK: a tool set for whole-genome association and population-based linkage analyses. Am J Hum Genet 2007;81(3):559-75.
27. Chang CC, Chow CC, Tellier LC, et al. Second-generation PLINK: rising to the challenge of larger and richer datasets. Gigascience 2015;4:7.
28. Zheng Z, Liu S, Sidorenko J, et al. Leveraging functional genomic annotations and genome coverage to improve polygenic prediction of complex traits within and between ancestries. Nat Genet 2024;56(5):767-77.
29. Craig JE, Han X, Qassim A, et al. Multitrait analysis of glaucoma identifies new risk loci and enables polygenic prediction of disease susceptibility and progression. Nat Genet 2020;52(2):160-6.
30. James G, Witten D, Hastie T, Tibshirani R. An Introduction to Statistical Learning with Applications in R, 1st ed. New York, NY: Springer, 2009; 426 p.
31. Chen T, Guestrin C. XGBoost: A Scalable Tree Boosting System. Proceedings of the 22nd ACM SIGKDD International Conference on Knowledge Discovery and Data Mining. San Francisco, California, USA: Association for Computing Machinery, 2016.
32. Lundberg SM, Erion G, Chen H, et al. From local explanations to global understanding with explainable AI for trees. Nature Machine Intelligence 2020;2(1):56-67.
33. Gao XR, Chiariglione M, Qin K, et al. Explainable machine learning aggregates polygenic risk scores and electronic health records for Alzheimer's disease prediction. Scientific Reports 2023;13(1):450.
34. He W, Lee SS, Diaz Torres S, et al. Predictive Power of Polygenic Risk Scores for Intraocular Pressure or Vertical Cup-Disc Ratio. JAMA Ophthalmol 2025;143(1):15-22.
35. Tran JH, Kang J, Han E, et al. Use of Diagnostic Codes for Primary Open-Angle Glaucoma Polygenic Risk Score Construction in Electronic Health Record-Linked Biobanks. Am J Ophthalmol 2024;267:204-12.
36. Sekimitsu S, Ghazal N, Aziz K, et al. Primary Open-Angle Glaucoma Polygenic Risk Score and Risk of Disease Onset: A Post Hoc Analysis of a Randomized Clinical Trial. JAMA Ophthalmol 2024;142(12):1132-9.
37. Singh RK, Zhao Y, Elze T, et al. Polygenic Risk Scores for Glaucoma Onset in the Ocular Hypertension Treatment Study. JAMA Ophthalmol 2024;142(4):356-63.
38. Zhao H, Pasquale LR, Zebardast N, et al. Screening by Glaucoma Polygenic Risk Score to Identify Primary Open-Angle Glaucoma in Two Biobanks: an Interim Report. Investigative Ophthalmology & Visual Science 2024;65(7):1010-.
39. Prive F, Arbel J, Vilhjalmsson BJ. LDpred2: better, faster, stronger. Bioinformatics 2021;36(22-23):5424-31.
40. MacGregor S, Ong JS, An J, et al. Genome-wide association study of intraocular pressure uncovers new pathways to glaucoma. Nat Genet 2018;50(8):1067-71.
41. Martschenko DO, Wand H, Young JL, Wojcik GL. Including multiracial individuals is crucial for race, ethnicity and ancestry frameworks in genetics and genomics. Nat Genet 2023;55(6):895-900.
42. Gao XR, Chiariglione M, Arch AJ. Whole-exome sequencing study identifies rare variants and genes associated with intraocular pressure and glaucoma. Nature Communications 2022;13(1):7376.

430 **Figure legends**

431 **Figure 1. Receiver Operating Characteristic Curves Predicting POAG Using Polygenic Risk Scores**

432 Receiver operating characteristic curves illustrating the predictive performance of polygenic risk scores
433 (PRSs) for primary open-angle glaucoma (POAG) in (A) the UK Biobank cohort and (B) the Mexican
434 American Glaucoma Genetic Study (MAGGS) cohort. In both cohorts, models including age, sex, and
435 PRSs significantly improved the area under the curve (AUC) compared to the baseline models with only
436 age and sex.

437 Abbreviations: IOP, intraocular pressure; RNFL, retinal nerve fiber layer; VCDR, vertical cup-to-disc ra-
438 tio.

439

440 **Figure 2. Association Between Polygenic Probability Risk Score Deciles and POAG Risk**

441 Odds ratios (ORs) for primary open-angle glaucoma (POAG) across deciles of the polygenic probability
442 risk score (PPRS) in (A) the UK Biobank cohort and (B) the Mexican American Glaucoma Genetic Study
443 (MAGGS) cohort. The lowest decile (Decile 1) serves as the reference group. Error bars represent 95%
444 confidence intervals (CIs). There is a clear trend of increasing POAG risk with higher PPRS deciles,
445 demonstrating strong risk stratification capabilities of PPRS in both cohorts.

446

447 **Supplementary Figure 1. Manhattan Plot Displaying the –log10(*P* values) for the Association Be-**
448 **tween RNFL Thickness and Genome-wide Genetic Variants**

449 Solid and dotted horizontal lines represent genome-wide significant associations ($P < 5 \times 10^{-8}$) and sug-
450 gestive associations ($P < 5 \times 10^{-5}$), respectively. Genetic variants are plotted by genomic position.

451

452 **Supplementary Figure 2. SHAP Feature Importance for XGBoost Models**

453 Bar charts illustrating feature importance, as evaluated via SHapley Additive exPlanations (SHAP) val-
454 ues, for the (A) UK Biobank and (B) Mexican American Glaucoma Genetic Study (MAGGS) cohorts.
455 The y-axis displays the ranked features, and the x-axis shows the average impact on the model's output.
456 PRS-POAG, PRS-IOP, PRS-VCDR, and PRS-RNFL were SBayesRC-derived.

457 Abbreviations: IOP, intraocular pressure; RNFL, retinal nerve fiber layer; VCDR, vertical cup-to-disc ra-
458 tio.
459
460

461 **Table 1. Sample Characteristics**
462

	UK Biobank (n = 324,713)		**MAGGS** (n = 4,549)	
	Controls (322,545)	Cases (2,168)	Controls (4,274)	Cases (275)
Age (yrs, SD)	57.1 (8.0)	63.0 (5.7)	56.1 (10.2)	66.4 (11.1)
Female (%)	54.3	48.4	59.2	52.4

463 Abbreviation: MAGGS, Mexican American Glaucoma Genetic Study; SD: standard deviation.
464
465

466 **Table 2. Single-PRS Logistic Regression Results**
467
468 (a) UK Biobank participants

	OR (95% CI)	*P* value	AUC (95% CI)
PRS-POAG-C+T	1.71 (1.64, 1.79)	8.71×10^{-141}	0.76 (0.75, 0.77)
PRS-POAG	2.14 (2.05, 2.24)	8.54×10^{-269}	0.79 (0.78, 0.80)
PRS-IOP	2.08 (2.00, 2.17)	1.04×10^{-248}	0.79 (0.79, 0.80)
PRS-VCDR	1.61 (1.54, 1.68)	9.50×10^{-107}	0.75 (0.74, 0.76)
PRS-RNFL	0.92 (0.89, 0.96)	2.52×10^{-4}	0.72 (0.71, 0.73)

469 (b) MAGGS[†] participants

	OR (95% CI)	*P* value	AUC (95% CI)
PRS-POAG-C+T	1.64 (1.44, 1.88)	1.68×10^{-13}	0.76 (0.73, 0.79)
PRS-POAG-MTAG	1.44 (1.24, 1.60)	1.17×10^{-7}	0.75 (0.72, 0.78)
PRS-POAG	1.82 (1.59, 2.08)	2.79×10^{-18}	0.77 (0.74, 0.80)
PRS-IOP	1.45 (1.27, 1.65)	1.66×10^{-8}	0.75 (0.72, 0.78)
PRS-VCDR	1.90 (1.66, 2.17)	1.39×10^{-20}	0.78 (0.75, 0.81)
PRS-RNFL	0.85 (0.74, 0.96)	0.011	0.75 (0.72, 0.77)

470 Results of single-PRS logistic regression analyses, adjusted for age and sex. [†]Unrelated MAGGS partici-
471 pants (n = 4,108) were used. PRS-POAG, PRS-IOP, PRS-VCDR, and PRS-RNFL were SBayesRC-de-
472 rived. To prevent potential data leakage, MTAG-derived PRS (based on Craig et al.'s summary statistics,
473 which used UK Biobank data) was not applied to UK Biobank participants. PRS-POAG-MTAG was ex-
474 clusively applied to MAGGS study participants.

475 Abbreviations: C+T, clumping and thresholding; IOP, intraocular pressure; MAGGS, Mexican American
476 Glaucoma Genetic Study; OR, odds ratio; PRS, polygenic risk score; POAG, primary open-angle glau-
477 coma; RNFL, retinal nerve fiber layer thickness; VCDR, vertical cup-to-disc ratio.
478
479

480 **Table 3. Multiple Logistic Regression Results**
481

	UK Biobank		MAGGS†	
	OR (95% CI)	*P* value	OR (95% CI)	*P* value
PRS-POAG	1.59 (1.51, 1.67)	1.23×10^{-74}	1.40 (1.18, 1.65)	7.63×10^{-5}
PRS-IOP	1.63 (1.55, 1.71)	5.37×10^{-89}	1.15 (0.99, 1.35)	0.07
PRS-VCDR	1.28 (1.23, 1.34)	1.99×10^{-27}	1.64 (1.42, 1.90)	2.04×10^{-11}
PRS-RNFL	0.94 (0.90, 0.98)	0.002	0.85 (0.74, 0.97)	0.016

482 Results of multiple logistic regression analyses, adjusted for age and sex, assessing the combined associa-
483 tion of polygenic risk scores (PRSs) with primary open-angle glaucoma. †Unrelated MAGGS participants
484 (n = 4,108) were used. PRS-POAG, PRS-IOP, PRS-VCDR, and PRS-RNFL were SBayesRC-derived.

485 Abbreviations: IOP, intraocular pressure; MAGGS, Mexican American Glaucoma Genetic Study; OR,
486 odds ratio; PRS, polygenic risk score; POAG, primary open-angle glaucoma; RNFL, retinal nerve fiber
487 layer thickness; VCDR, vertical cup-to-disc ratio.
488
489

490 **Figure 1. Receiver Operating Characteristic Curves Predicting POAG Using Polygenic Risk Scores**

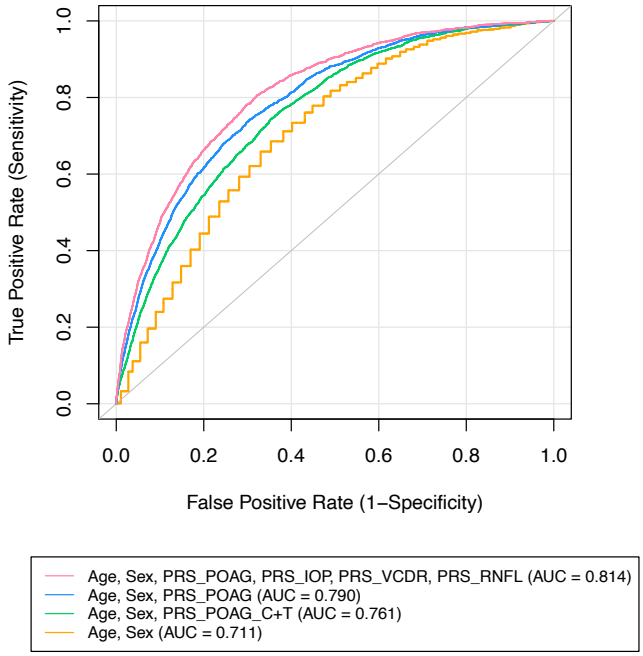

491
492 (a) UK Biobank participants

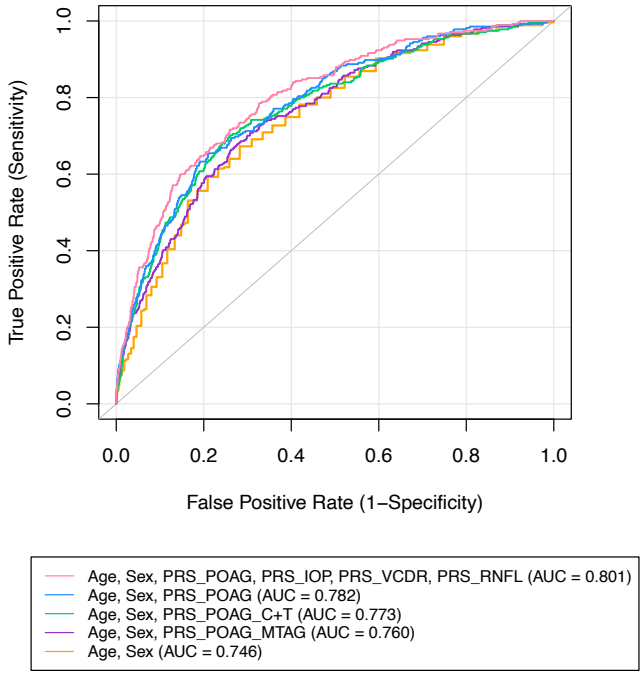

493
494 (b) MAGGS participants

495
496 **Figure 2. Association Between Polygenic Probability Risk Score Deciles and POAG Risk**

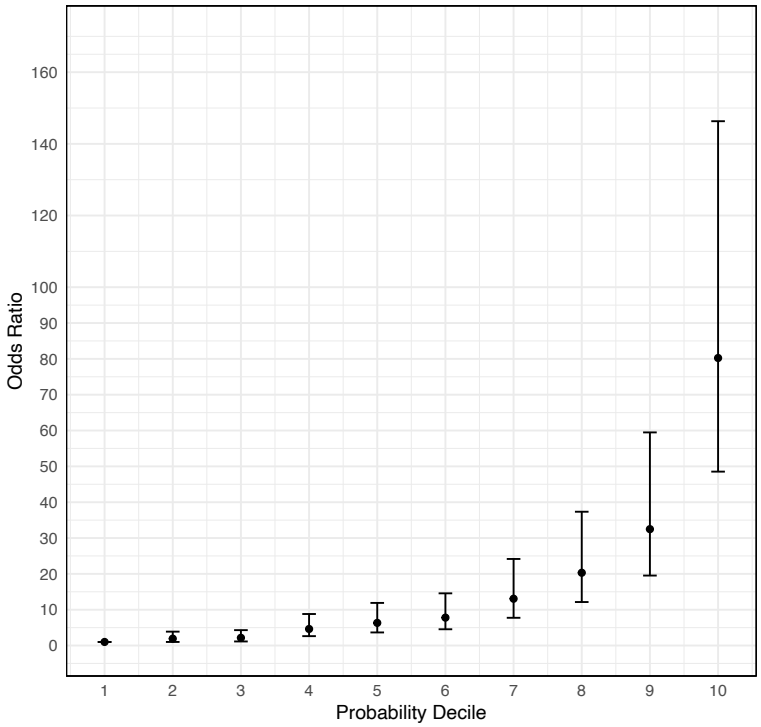

497
498 (a) UK Biobank participants

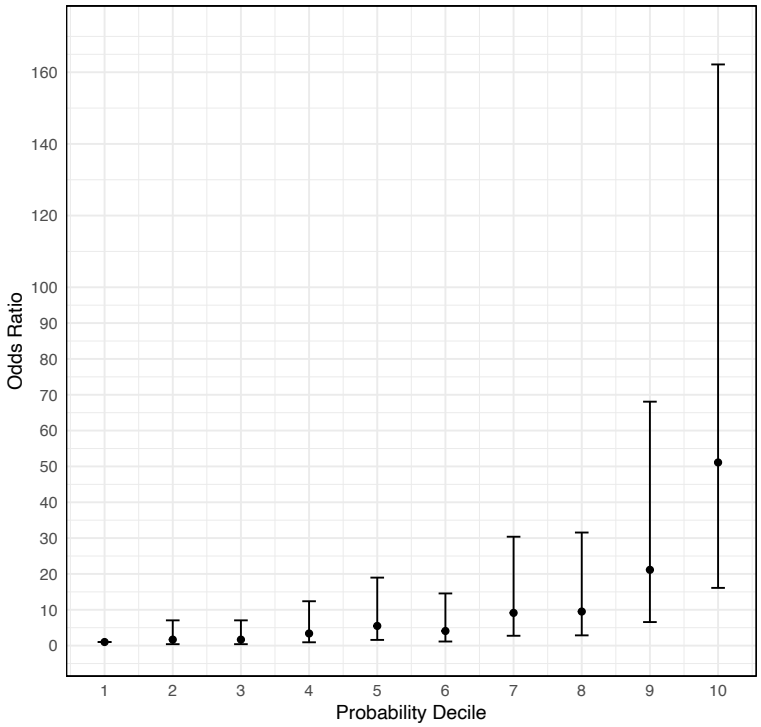

499
500 (b) MAGGS participants

Supplementary Table 1. Variance Inflation factors for polygenic risk scores in our logistic regression models

(a) UK Biobank

Age	Sex	PRS-POAG	PRS-IOP	PRS-VCDR	PRS-RNFL
1.002	1.002	1.347	1.240	1.112	1.003

(b) MAGGS[†]

Age	Sex	PRS-POAG	PRS-IOP	PRS-VCDR	PRS-RNFL
1.024	1.006	1.555	1.371	1.166	1.004

Displayed are the variance inflation factors for the polygenic risk scores (PRSs) used in our logistic regression analyses of a) UK Biobank; b) MAGGS. [†]Unrelated MAGGS participants were used. PRS-POAG, PRS-IOP, PRS-VCDR, and PRS-RNFL were SBayesRC-derived.

Abbreviations: IOP, intraocular pressure; MAGGS, Mexican American Glaucoma Genetic Study; PRS, polygenic risk score; POAG, primary open-angle glaucoma; RNFL, retinal nerve fiber layer thickness; VCDR, vertical cup-to-disc ratio.

514 **Supplementary Table 2. Number of POAG Cases in Each Decile Category**
515
516 (a) UK Biobank

	Predicted Probability Risk Score Decile									
	1	2	3	4	5	6	7	8	9	10
POAG, n (%)	13 (0.60)	25 (1.15)	28 (1.29)	60 (2.77)	82 (3.78)	101 (4.66)	169 (7.80)	262 (12.08)	417 (19.23)	1011 (46.63)

517
518
519 (b) MAGGS

	Predicted Probability Risk Score Decile									
	1	2	3	4	5	6	7	8	9	10
POAG, n (%)	3 (1.09)	5 (1.82)	5 (1.82)	10 (3.64)	16 (5.82)	12 (4.36)	26 (9.45)	27 (9.82)	56 (20.36)	115 (41.82)

520
521
522

523 **Supplementary Figure 1. Manhattan Plot Displaying the –log10(*P* values) for the Association Be-**
524 **tween RNFL Thickness and Genome-wide Genetic Variants**
525

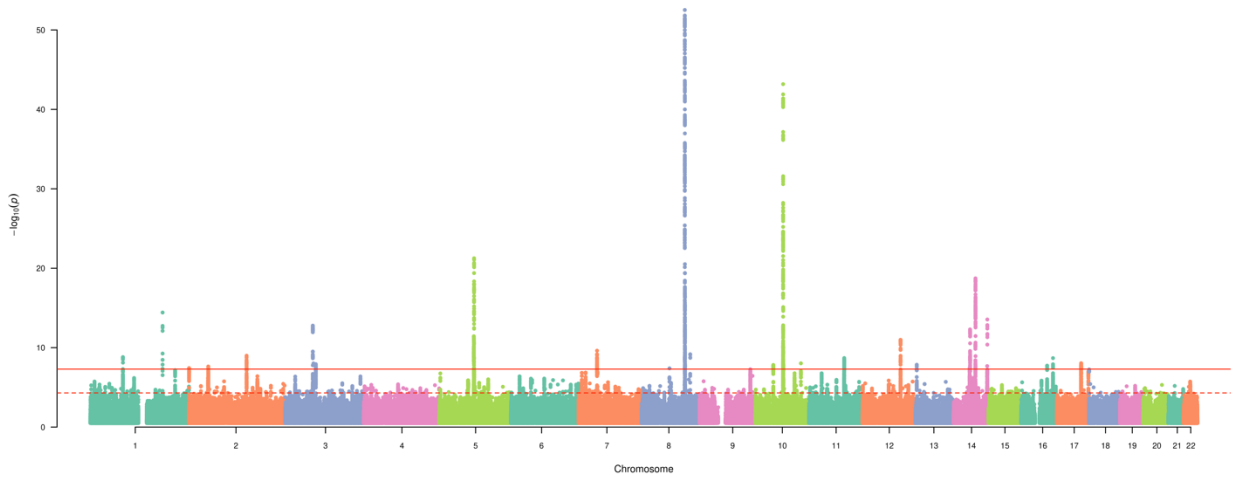

526
527
528

529

Supplementary Figure 2. SHAP Feature Importance for XGBoost Models

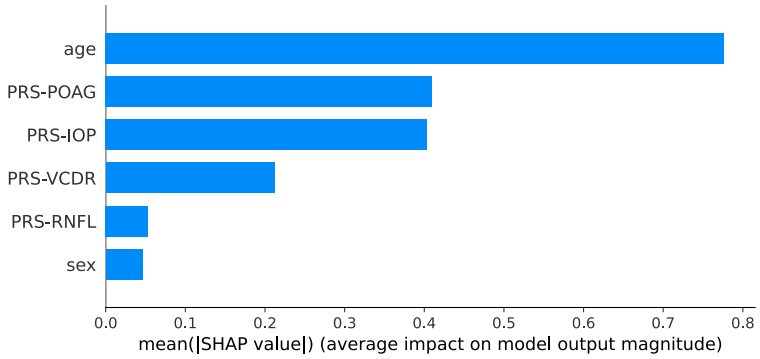

(a) UK Biobank participants

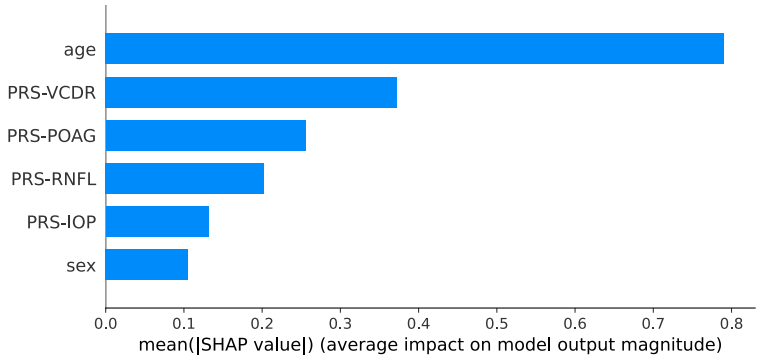

(b) MAGGS participants